

# Detections of Directional Dynamic Triggering in Intraplate Regions of the United States

Vivian Tang<sup>\*1,2</sup>, Kevin Chao<sup>1,3</sup>, and Suzan van der Lee<sup>1,3,4</sup>

## ABSTRACT

We report tremor or local earthquake signals that occurred during the propagation of Love and Rayleigh waves from the 2012  $M_w$  8.6 Sumatra earthquake in three intraplate regions: Yellowstone, central Utah, and Raton basin (Colorado). These surface waves likely also dynamically triggered seismic activity along the western boundary of the North American plate, and did not trigger seismic activity in the central and eastern United States. We report additional potential dynamic triggering in the three aforementioned intraplate regions by surface waves from 37 additional large earthquakes, recorded between 2004 and 2017. These surface waves' transient stresses generally appear to trigger tremor in seismically, volcanically, and hydrothermally active regions, such as Yellowstone, if the waves also arrive from favorable directions. These stresses do not appear to be decisive factors for triggering local earthquakes reported for the Raton basin and central Utah, whereas, surface waves' incidence angles do appear to be important there.

## KEY POINTS

- Three intraplate U.S. sites show dynamic triggering by surface waves from large remote earthquakes.
- Peak dynamic stress is  $> 10$  kPa when Yellowstone tremor triggered but seems random for triggered earthquakes.
- Dynamic triggering seems to be favored for a narrow range of surface-wave incidence angles at each site.

## Supplemental Material

## INTRODUCTION

Far-field surface waves of large magnitude earthquakes can dynamically trigger seismic events such as small, local earthquakes (Prejean *et al.*, 2004) and tectonic tremor (Gomberg *et al.*, 2008; Peng *et al.*, 2009), even when associated transient stresses peak as low as 1 or 2 kPa (Peng and Gomberg, 2010; Brodsky and van der Elst, 2014). Figure 1 shows two examples of such events. Understanding the conditions under which surface waves can and do trigger local seismicity requires observations as reported here and may provide insight into the physics of earthquake nucleation (Kato *et al.*, 2013). In addition, determining the frequency and conditions under which triggered seismic events occur will lead to a better understanding of seismicity, in general.

Triggered tremor and triggered earthquakes have been observed at tectonic plate boundaries and major faulting systems worldwide. Along the western boundary of the North American plate, many studies have reported dynamic triggering of local earthquakes (Velasco *et al.*, 2008; Cerda *et al.*, 2011; Aiken

and Peng, 2014; Brodsky and Van der Elst, 2014; Linville *et al.*, 2014; Hill and Prejean, 2015) and tectonic tremor (Rubinstein *et al.*, 2009; Chao *et al.*, 2012, 2017; Gomberg and Prejean, 2013; Aiken and Peng, 2014). Fewer studies reported triggered seismic events in the continental interior of the United States (Prejean *et al.*, 2004; Freed, 2005; Van der Elst *et al.*, 2013; Velasco *et al.*, 2016). Within the intraplate interior of North America, the hydrothermally, volcanically, and the seismically active region around Yellowstone National Park experienced dynamic triggering following the 2002 Denali earthquake (Husen *et al.*, 2004), as did the Wasatch fault zone in Utah (Pankow *et al.*, 2004). Van der Elst *et al.* (2013) report delayed dynamic triggering of local earthquakes in regions of anthropogenic seismicity, such as the Raton basin, Colorado, Prague of Oklahoma, and Snyder, Texas, for three days following the 2011  $M_w$  9.1 Tohoku and the 2010  $M_w$  8.8 Chile earthquakes. Velasco *et al.* (2016) also found triggered earthquakes in Texas as well as the Coso region in California, respectively, following the same two earthquakes. The number of dynamically triggered events reported in the literature keeps growing (Canitano *et al.*, 2019), suggesting that

1. Department of Earth and Planetary Sciences, Northwestern University, Evanston, Illinois, U.S.A., <https://orcid.org/0000-0002-2323-0613> (VT); <https://orcid.org/0000-0001-8108-1890> (KC); <https://orcid.org/0000-0003-1884-1185> (SvdL);

2. Now at Department of Civil and Environmental Engineering, University of Illinois Urbana-Champaign, Urbana, Illinois, U.S.A.; 3. Northwestern Institute on Complex Systems (NICO), Northwestern University, Evanston, Illinois, U.S.A.; 4. Center for Interdisciplinary Exploration and Research in Astrophysics (CIERA), Northwestern University, Evanston, Illinois, U.S.A.

\*Corresponding author: [viviant@illinois.edu](mailto:viviant@illinois.edu)

**Cite this article as** Tang, V., K. Chao, and S. van der Lee (2021). Detections of Directional Dynamic Triggering in Intraplate Regions of the United States, *Bull. Seismol. Soc. Am.* **XX**, 1–18, doi: [10.1785/0120200352](https://doi.org/10.1785/0120200352)

© Seismological Society of America

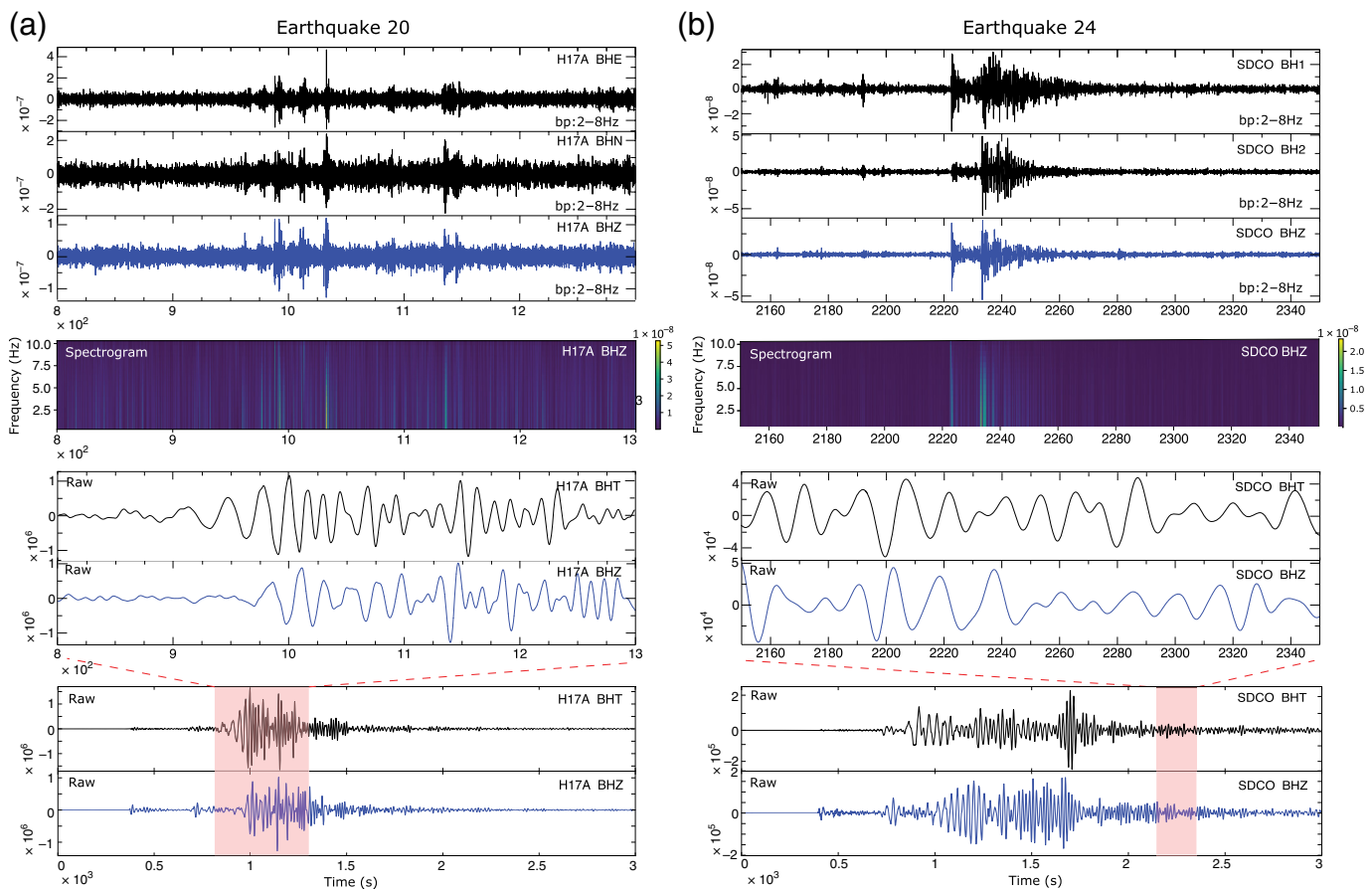


**Figure 1.** Examples of the dynamic triggering of (a) triggered tremor and (b) triggered earthquakes during the surface wavetrains of earthquakes 20 (20 March 2012  $M_w$  7.5 Mexico) and 24 (5 September 2012  $M_w$  7.6 Costa Rica), respectively. From bottom to top: Raw, vertical-, and transverse-component seismogram; Same as in bottom frame but zoomed in to the pink-highlighted time window; Spectrogram of the band-passed zoomed-in, vertical-component seismogram; the band's corner frequencies are 2 and 8 Hz; the top three frames are band-passed vertical-, north-, and east-component seismograms of the zoomed-in time window. Y-axis units are in m/s for band-passed waveforms and count for raw data. The color version of this figure is available only in the electronic edition.

their quantity and pervasiveness can be expanded and exploited to study the conditions necessary for such triggering.

In this study, we expand the diversity of reported dynamically triggered seismicity by exploring and reporting additional activity in the continental, the intraplate interior of the United States, and we analyze the conditions that prevail during dynamic triggering from ever-increasing catalogs of triggered events. To do the former, we first interactively investigated all broadband seismograms of the 2012  $M_w$  8.6 Sumatra earthquake recorded in the United States. Second, we investigated seismograms of 38  $M_w > 7$  earthquakes recorded in three intraplate regions found in step one to contain signals from triggered seismicity in records of the 2012  $M_w$  8.6 Sumatra earthquake. Finally, we discuss to what extent peak dynamic stress estimates, as well as other parameters, appear important for triggering the reported tremor and earthquakes.

## DATA MINING FOR POTENTIALLY TRIGGERED SEISMIC EVENTS: DATA AND METHODS

### The 2012 $M_w$ 8.6 Sumatra earthquake

The 11 April 2012  $M_w$  8.6 Sumatra earthquake is the largest magnitude strike-slip earthquake recorded to date (Meng *et al.*, 2012), and, it radiated large-amplitude Love waves, with one of four radiation maxima oriented toward USArray (Rösler and Van der Lee, 2020). As Love waves hold considerable dynamic triggering potential (Peng and Gomberg, 2010; Hill, 2012; Castro

*et al.*, 2015; Bansal *et al.*, 2016, 2018; Chao and Obara, 2016; Johnson and Bürgmann, 2016; Kundu *et al.*, 2016; Chao and Yu, 2018), we searched for signals in USArray and other U.S. data from potentially dynamically triggered intraplate seismic events that occurred during the passage of surface waves from the 11 April 2012  $M_w$  8.6 Sumatra earthquake. Love waves can temporarily enhance shear stress on faults they propagate across. Van der Elst *et al.* (2013) examined dynamic triggering by this earthquake's surface waves in regions of anthropogenic seismicity and in two locations found an elevated number of local earthquakes during post teleseismic earthquake days. However, this elevated number was much smaller than that found following the 2011  $M_w$  9.1 Tohoku and the 2010  $M_w$  8.8 Chile earthquakes, which radiated stronger Rayleigh

waves. It may be unlikely that Love waves are a primary cause of triggering seismic activity in regions with little tectonic activity. Here, we are interested in the possible triggering of tectonic events and choose the 2012  $M_w$  8.6 Sumatra earthquake, with its high-amplitude Love waves, to help test this hypothesis.

## USArray data processing

During the 2012  $M_w$  8.6 Sumatra earthquake, all seismic components of EarthScope's USArray (see [Data and Resources](#)) were in place: The Transportable Array (TA), the Flexible Array (FA), the Reference Network, as well as cooperating regional networks, such as the University of Utah Regional Seismic Network (UU). The TA has been operating since 2004, methodically migrating from west to east across the United States before leaping to Alaska, where it is currently deployed. The TA, equipped with three-component broadband stations separated by, approximately, 70 km, is a large-scale seismic network. The FA consists of similar broadband stations that were deployed in smaller regions in more flexible geometries for limited durations by individual research teams. Here, we included data from USArray and other permanent and temporary seismic networks, such as the Advanced National Seismic System, that were recording in the United States during the first greater decade (hereafter, dodecade) of EarthScope (See [Data and Resources](#) for details).

For the 2012  $M_w$  8.6 Sumatra earthquake, we downloaded all available broadband seismograms recorded in the United States via Incorporated Research Institutions for Seismology, Data Services (see [Data and Resources](#) for details). The downloaded waveforms start 60 min before and end 180 min after the origin time of the earthquake. The raw waveforms were converted to ground velocity, by deconvolving with the instrument response. The waveforms were filtered with a 2–8 Hz band-pass filter, when searching for triggered tremor and triggered earthquakes. Frequency content above 8 Hz is not available or reliable for all stations, which have different instrumentation and sampling rates. Waveforms without high-frequency signals from local earthquakes or tremor were removed. The waveforms from the original orientations were rotated to radial, transverse components, when we estimated the peak dynamic shear stress.

## Criteria for identifying triggered tremor and triggered earthquakes

Signals from triggered earthquakes are similar to signals from small, local earthquakes and have visible *P*- and *S*-wave energy at frequencies above 5 Hz. To identify *P* and *S* waves, we examined three-component seismograms. Earthquake signals are only considered as potentially triggered when they occur during the propagation of the surface wavetrain and have a statistical probability of occurring during that time window of 3% or less. We consider an earthquake as possibly triggered ([Aiken and Peng, 2014](#)) if: (1) the earthquake occurs during the propagation of Love and Rayleigh wavetrains; (2) the earthquake signal has

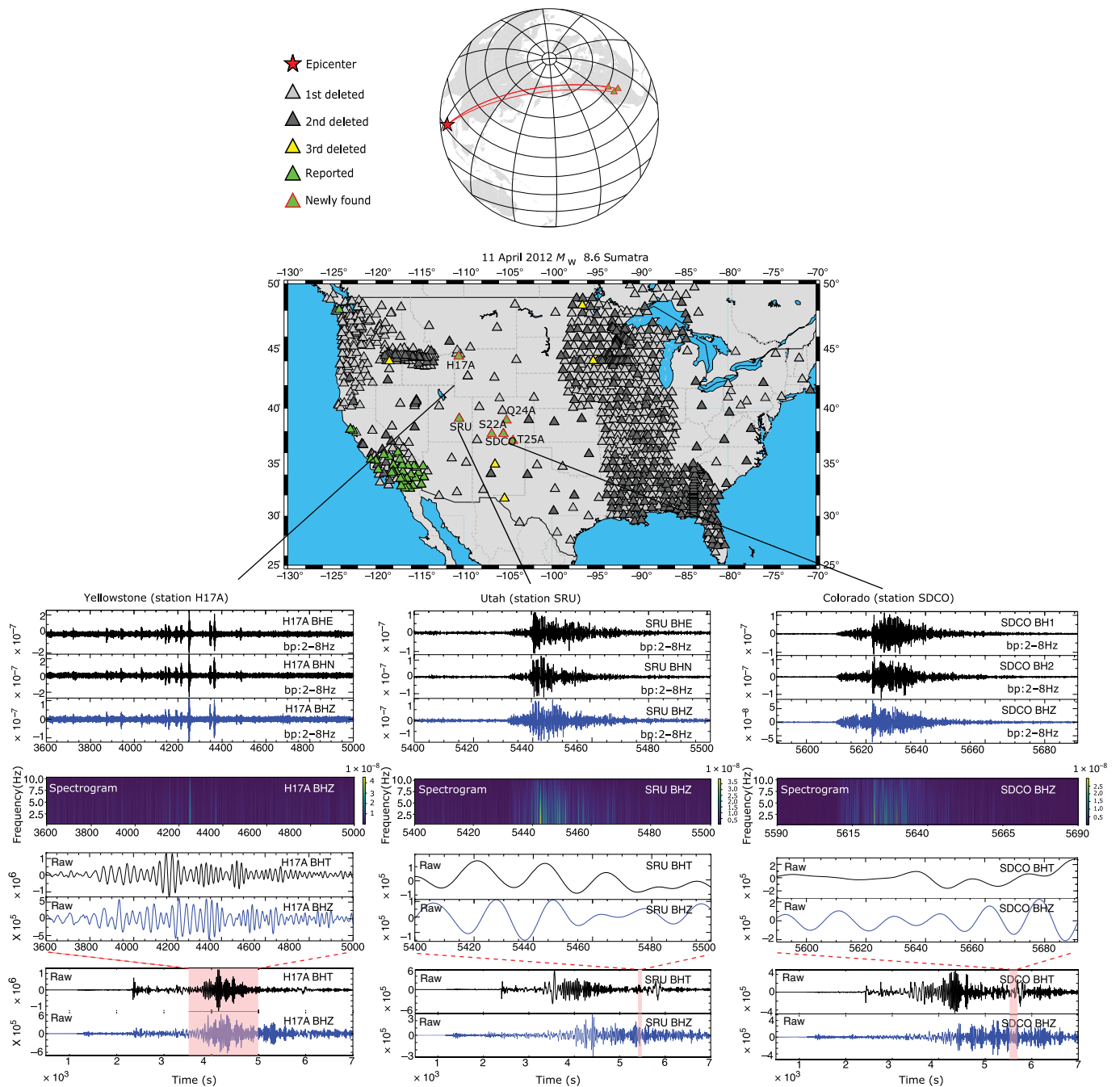
elevated power within the passband between 2 and 8 Hz; (3) the earthquake signal shows clear *P* and *S* waves above the noise level (Fig. 1b); (4) the earthquake signals come from local earthquakes rather than teleseismic aftershocks; and (5) there is little to no local activity within 24 hr before the examined time window. We checked the seismogram more than one day before and after the examined time window of potentially triggered signals, to make sure there is little or no local activity. If we found out there is a high local activity, we further examined longer time before and after the examined time window.

In addition, we excluded the possibility that the detected events occurred within the surface-wave windows by chance, because the frequency of detections within the examined surface windows exceeds the frequency expected from 20 yr of local background seismicity. We estimated the expected frequency by counting 20 yr of U.S. Geological Survey (USGS)-reported (see [Data and Resources](#)) earthquakes within 100 km of a station and in a magnitude bin one point higher than the estimated low magnitudes (below the catalog magnitude of completion) of the triggered events. We multiplied this by 10 and inferred the number of low-magnitude earthquakes that would occur on average within the surface-wave time window. The probability of a low-magnitude event occurring randomly within this time window is less than 3% for the Utah site, which is the most seismically active of the three study sites, and even less for the other two study sites.

Bursts of triggered tremor occur during surface wavetrains and can last for 5–30 min. To identify possibly triggered tremor, we use the following criteria ([Chao and Yu, 2018](#)): (1) tremor occurs during the propagation of Love and Rayleigh wavetrains; (2) tremor has dominant frequencies between 2 and 8 Hz; (3) tremor looks like a series of bursts, with a similar modulating frequency as that of the coeval surface waves (Fig. 1a); and (4) the tremor is either recorded by, at least, two nearby stations within, approximately, 50 km of each other ([Chao et al., 2019](#)) or has been activated by more than one large teleseismic earthquakes. Graphs of all signals selected as possibly triggered are provided in Figures S1–S8 (available in the supplemental material to this article).

## Earthquakes investigated

In addition to interactively examining seismograms of the 2012  $M_w$  8.6 Sumatra earthquake (Fig. 2) from over 1000 seismic stations, we examined seismograms from a subset of stations for 37 additional earthquakes with  $M_w > 7.0$  (Table 1), and one, slightly smaller foreshock. The subsets of stations were selected to be in three intraplate regions where surface waves from the 2012  $M_w$  8.6 Sumatra earthquake possibly triggered tremor or a local earthquake. The selected earthquakes not only had moment magnitudes ( $M_w$ ) greater than 7.0, they also had event depths less than 100 km and were, at least, 10° away ([Chao and Obara, 2016](#)) from the investigated station locations. Between 2004 and 2017, 175 earthquakes matched these criteria. For each location, we estimated the surface-wave amplitudes generated by the large earthquake's surface waves



using a magnitude–distance relationship (Chao *et al.*, 2013), and rejected earthquakes with estimated ground-velocity amplitudes below 0.1 mm/s. We use the ground velocity to estimate the associated change in shear stress  $\sigma$  as

$$\sigma = \mu \dot{u}/U,$$

in which  $\mu$  is the shear modulus,  $\dot{u}$  is the surface-wave ground velocity,  $U$  is the surface wave's group velocity, and  $\dot{u}/U$  approximates half the deviatoric strain (Chao and Obara, 2016). Using  $\mu = 35$  GPa as a representative shear modulus for the crust and  $U = 3.5$  km/s as a representative average group velocity, we estimate the peak shear stress in kPa to equal  $10^4 \times A$ , in which  $A$  is the peak ground velocity (PGV) in m/s. This implies

**Figure 2.** (Top) Map of USArray and affiliated stations (triangles) that recorded earthquake 21 (11 April 2012  $M_w$  8.6 Sumatra). Green-colored stations recorded signals from triggered events; all other-colored stations did not. (Bottom) Seismogram panels with the same layout as in Figure 1, showing data from each of the three intraplate regions where we report potentially triggered local events: tremor in Yellowstone (left), and earthquakes in Utah (center), and the Raton basin, Colorado (right). The color version of this figure is available only in the electronic edition.

that the 37 additional earthquakes we selected (Fig. 3) were estimated to cause dynamic-stress changes that exceeded 1 kPa. We then investigated whether seismicity occurred in the three identified locations during the propagation of these earthquakes'

TABLE 1

**Origin Times and Hypocenters of 38 Earthquakes of  $M_w \geq 7.0$ , along with Whether Their Surface Waves Potentially Triggered Tremor in Yellowstone (H17A) or Local Earthquakes in Central Utah (SRU), or the Raton Basin (SDCO)**

Number	Date (yyyy/mm/dd)	Longitude (°)	Latitude (°)	Depth (km)	$M_w$	H17A Tremor	SRU Earthquake	SDCO Earthquake
1	2004/12/23	161.25	-49.91	27.5	8.1	N/A	x	x
2	2004/12/26	94.26	3.09	28.6	9.0	N/A	x	x
3	2005/03/28	97.07	1.67	25.8	8.6	N/A	N/A	x
4	2006/04/20	167.05	60.89	12.0	7.6	N/A	x	x
5	2006/05/03	-173.47	-20.39	67.8	8.0	N/A	N/A	x
6	2006/11/15	154.33	46.71	13.5	8.3	N/A	x	x
7	2007/01/13	154.8	46.17	12.0	8.1	N/A	x	x
8	2007/04/01	156.34	-7.79	14.1	8.1	N/A	x	x
9	2007/08/15	-77.04	-13.73	33.8	8.0	N/A	Maybe	x
10	2007/09/12	100.99	-3.78	24.4	8.5	N/A	Maybe	x
11	2007/11/14	-70.62	-22.64	37.6	7.7	x	x	x
12	2008/05/12	104.10	31.44	12.8	7.9	Maybe	x	x
13	2009/05/28	-87.17	16.5	29.0	7.3	x	Maybe	x
14	2009/09/29	-171.97	-15.13	18.5	8.1	x	x	x
15	2009/10/07	166.01	-11.86	41.7	7.8	x	x	x
16	2010/02/27	-72.93	-36.15	28.1	8.8	x	x	x
17	2010/04/04	-115.39	32.31	12.8	7.2	x	x	x
18	2011/03/11	143.05	37.52	20.0	9.1	x	x	x
19	2011/06/24	-171.77	52.09	74.2	7.3	x	x	x
20	2012/03/20	-98.39	16.6	15.4	7.5	Yes	x	x
21	2012/04/11	92.82	2.35	45.6	8.6	Maybe	Yes	Yes
22	2012/04/12	-112.76	28.57	15.8	7.0	x	x	x
23	2012/08/27	-89.17	12.02	12.0	7.3	x	x	Yes
24	2012/09/05	-85.64	10.00	29.7	7.6	x	Yes	Yes
25	2012/10/28	-132.06	52.61	12.0	7.8	x	x	x
26	2012/11/07	-92.43	14.11	21.3	7.4	x	x	x
27	2013/01/05	-134.97	55.69	13.8	7.5	x	N/A	x
28	2013/02/06	165.21	-11.18	20.2	7.9	x	x	x
29	2014/04/01	-70.81	-19.70	21.6	8.1	x	x	x
30	2014/04/03	-70.6	-20.43	28.7	7.7	x	Maybe	x
31	2014/04/18	-101.25	17.55	18.9	7.3	x	N/A	x
32	2014/10/14	-88.45	12.33	40.8	7.3	x	x	x
33	2015/09/16	-72.09	-31.13	17.4	8.3	x	x	x
34	2016/04/16	-80.25	-0.12	22.3	7.8	x	x	x
35	2016/12/17	153.76	-5.55	52.8	7.9	x	x	x
36	2017/07/17	169.78	54.13	23.2	7.7	x	x	x
37	2017/09/08	-94.62	15.34	50.2	8.2	Maybe	x	x
38	2017/09/19	-98.62	18.51	52.7	7.1	x	x	x

Yes, a local event was identified; Maybe, a potentially triggered event was identified; x, no event signals were identified; N/A, no data available.

surface waves. We list all selected earthquakes in Table 1 and number them for easy reference. The 2012 Sumatra earthquake is earthquake 21. Earthquake 30 had a smaller  $M_w$  6.5 foreshock (not listed in Table 1) whose surface waves also potentially triggered a local earthquake in central Utah.

## DATA MINING FOR POTENTIALLY TRIGGERED SEISMIC EVENTS: RESULTS

### Observations of potentially triggered seismic events following the 2012 $M_w$ 8.6 Sumatra earthquake: Overview and western plate boundary

After visual examination of radial, transverse, and vertical components of 1021 seismograms of the 2012 Sumatra

earthquake (Fig. 2), we rejected 617 seismograms, because they exhibited either no high-frequency energy in the surface-wave window or contained data gaps, calibrations, mass centerings, instrument- or site-specific signals, or other nontectonic signals (Marciello and MacCarthy, 2020). Next, we visually inspected the surface-wave windows in the remaining 404 candidate seismograms for this earthquake in one or more frequency bands (i.e., 2–8 Hz band-pass or 5 Hz high-pass filter). We identified signals from local earthquakes or from tremor, if they met the pertinent criteria outlined in the [Criteria for Identifying Triggered Tremor and Triggered Earthquakes](#) section. Of these 404 seismograms, 47 candidates had signals that met the criteria for being from potentially dynamically triggered events. The rest

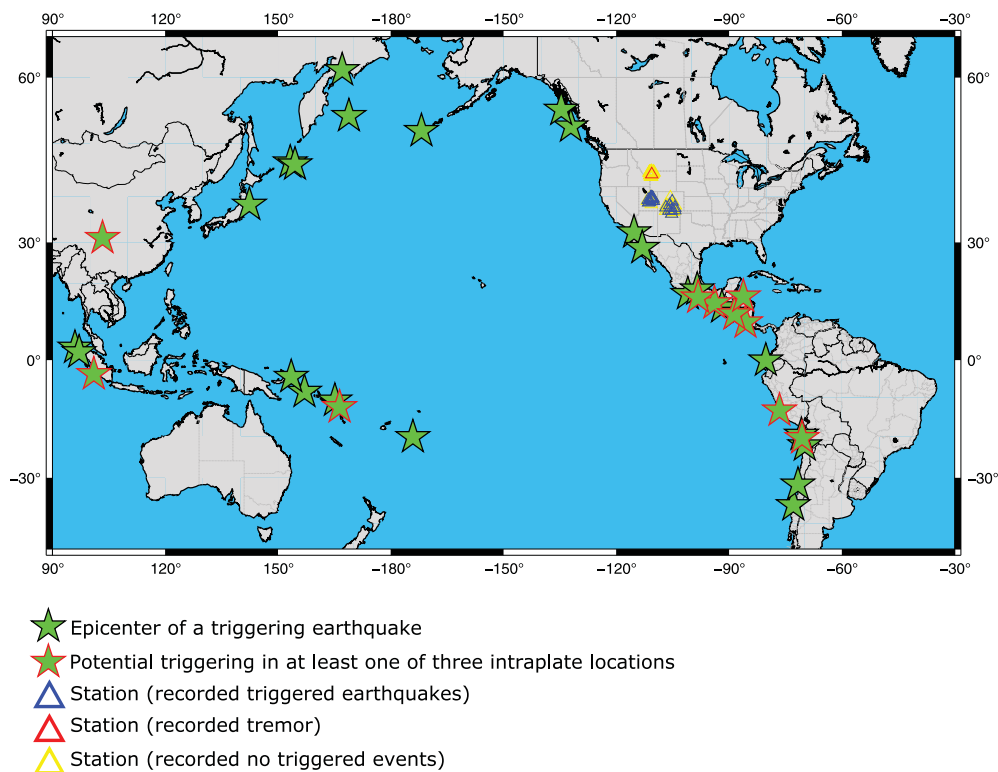


**Figure 3.** Map of epicenters of 38 large triggering earthquakes (green stars) and stations (triangles) whose data were examined for triggered events. Blue stations recorded, at least, one potentially triggered earthquake. The red station (H17A) recorded, at least, one potentially triggered tremor. Nearby yellow stations did not show signals from triggered events above the noise level. Epicenters with red outlines are associated with potential triggering in, at least, one of three intraplate locations: Yellowstone, Utah, and the Raton basin, Colorado.

of the seismograms contained some type of high-frequency signal or noise in the surface window that neither qualified as a tremor nor as an earthquake signal. About 36 out of these 47 candidates were observed along the western plate boundary (Fig. 2 and Table S1), where triggered events had previously been observed for other teleseismic earthquakes (Peng *et al.*, 2009; Chao *et al.*, 2012; Castro *et al.*, 2015, 2017).

### Intraplate triggering following the 2012 $M_w$ 8.6 Sumatra earthquake: Western United States

From detailed inspections of the remaining 11 candidates for newly discovered dynamic triggering east of the plate boundary, we rejected a further five. These rejections are based on the instrument- or site-specific noise, including the frequent occurrence of similar signals before and after the surface-wave window in regions that are seismically relatively quiescent. One of the six remaining signals represents a possibly dynamically triggered local earthquake (Fig. 2) in central Utah (station SRU).

Four of the six signals represent a dynamically triggered earthquake (Fig. 2) in Colorado (stations SDCO, T25A, Q24A, and S22A). Van der Elst *et al.* (2013) included this detection at station T25A in his three-day catalog of seismicity that followed the 11 April 2012  $M_w$  8.6 Sumatra earthquake.

Because of its longer deployment, we selected SDCO as a representative station for searching for dynamically triggered earthquakes during surface wavetrains from additional large earthquakes.

The final one of the six remaining signals possibly represents dynamically triggered tremor (Fig. 2) in Yellowstone (station H17A). However, several signals with comparable time progressions and bandwidth were recorded by the station in the hours leading up to the Sumatra earthquake, whereas, other stations about 10–20 km north of H17A did not record the signal, suggesting a possibly shallow source. In addition to being tectonically active, Yellowstone is also volcanically and hydrothermally active (Vandemeulebrouck *et al.*, 2013; Hurwitz *et al.*, 2014; Huang *et al.*, 2015). Station H17A is located within the Yellowstone Caldera.

### Absence of triggering following the 2012 $M_w$ 8.6 Sumatra earthquake: Central and eastern United States

The seismograms of the 2012 Sumatra earthquake that we examined were recorded at a dense collection of seismic stations (Fig. 2), including a Midwestern swath of TA and FA stations. At this time, the largest distance between two neighboring stations in the United States, away from TA and FA stations, was around 200 km. Each seismogram recorded in the central and eastern United States (CEUS) was inspected in different frequency bands, and all were rejected as not having recorded dynamically triggered seismicity. Likewise, Van der Elst *et al.* (2013) examined dynamic triggering by this earthquake's surface waves in regions of anthropogenic seismicity and found virtually no triggering in the CEUS, including at sites of anthropogenic seismicity in Texas, Arkansas, and Ohio. However, they did find a moderate surge in seismic activity in a wastewater injection area in Oklahoma (near stations V34A and V35A) and in Colorado (near stations SDCO and T25A) during the days that followed the Sumatra earthquake. Bockholt *et al.* (2014) report finding neither ambient nor triggered tremor around the Reelfoot fault in northern Tennessee during surface wave propagation from 11 large additional

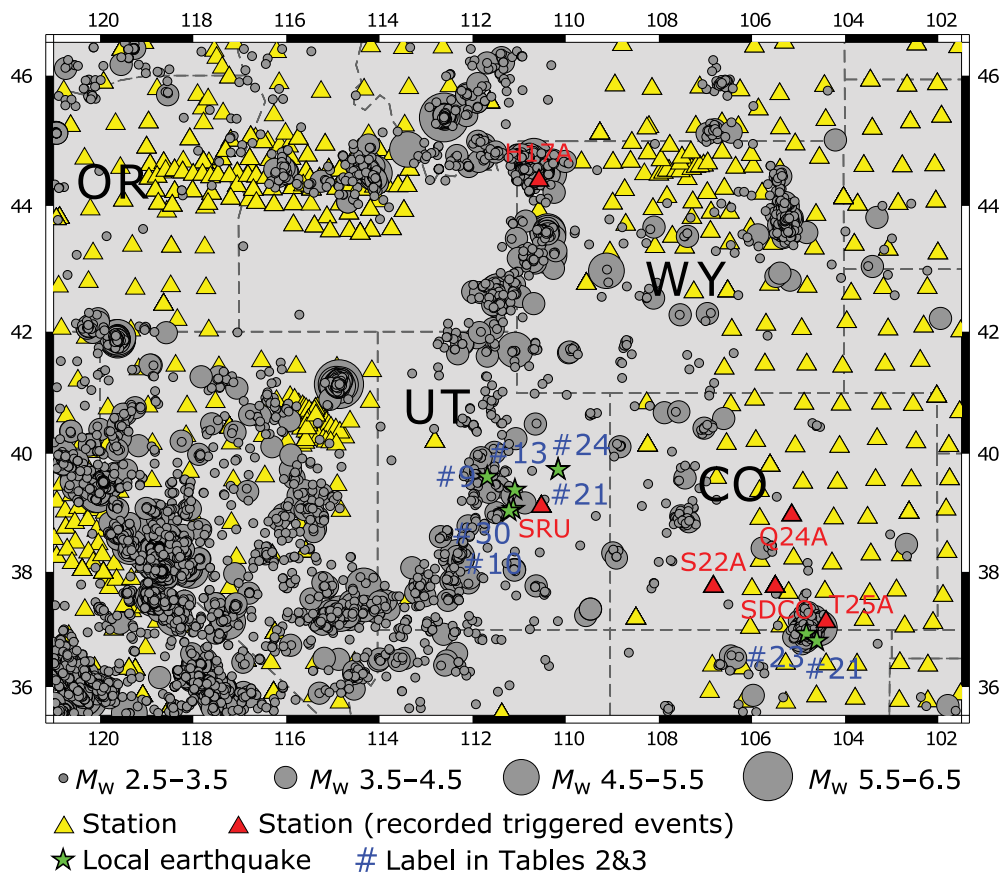


**Figure 4.** Map of earthquakes (gray circles) from 2004 to 2017 in Yellowstone, Utah, and Colorado from the U.S. Geological Survey (see [Data and Resources](#)). The size of the gray circles depends on the magnitude of the earthquake. Red triangles are stations for which we detected, at least, one potentially triggered local event. Green stars represent epicenters of the local earthquake potentially triggered by surface waves from the teleseismic earthquakes (blue number sign) in Tables 2 and 3. The color version of this figure is available only in the electronic edition.

earthquakes. Our analysis extends and confirms that there was virtually no dynamic triggering of tectonic seismic activity across all of the CEUS during the passage of surface waves from the 2012  $M_w$  8.6 Sumatra earthquake. There is relatively not active seismicity in CEUS; therefore, it may be less possible to experience triggered seismic events.

### Observations of potential dynamic triggering following 37 additional large earthquakes

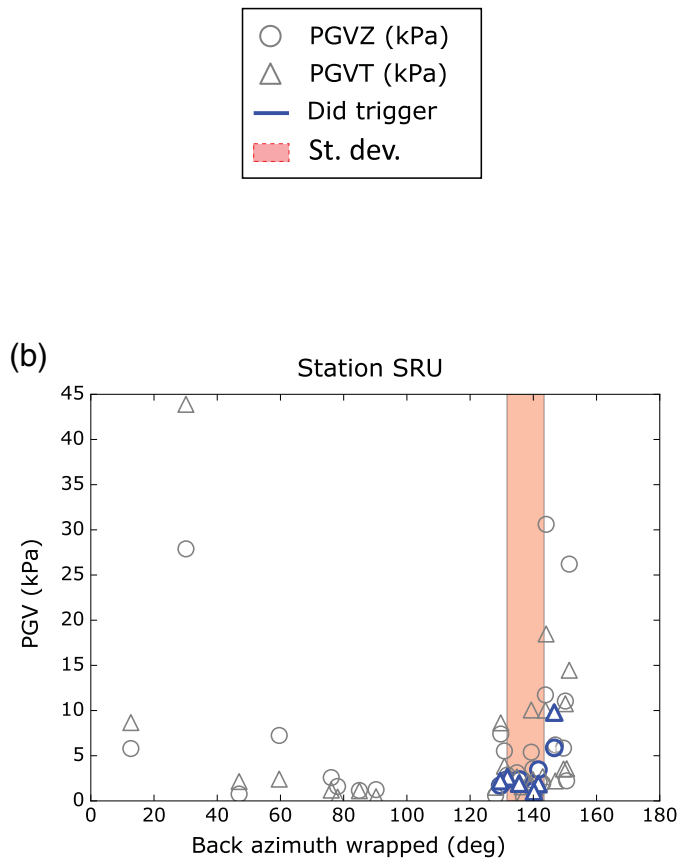
We examined seismograms recorded at the three intraplate locations represented by stations H17A, SRU, and SDCO, from 37 additional large earthquakes. With some of these earthquakes being recorded by a subset of the stations (H17A, SRU, and SDCO), we obtained 97 additional seismograms to examine. Within these 97 seismograms and for seven of the 38 earthquakes in total, we found possible dynamically triggered events recorded within the surface-wave arrival window (Figs. S2–S9). We also examined seismograms at nearby stations for each newly found potentially triggered event. Using

observations of the same local events at nearby stations and through picking P- and S-wave arrival times, we were able to locate eight local events (Fig. 4). We estimated peak dynamic shear stress from the vertical- and transverse-component ground-velocity seismograms of all 38 earthquakes and plotted them versus back azimuth in Figure 5. In the [Observations of Triggered Tremor in Yellowstone \(H17A Station\)](#), [Observations of Triggered Earthquakes in Central Utah \(SRU Station\)](#) and [Observations of Triggered Earthquakes in Colorado \(SDCO station\)](#) section, we discuss these new detections (Figs. 6 and 7), in detail, for each of the three intraplate locations.

### Observations of triggered tremor in Yellowstone (H17A station)

Station H17A station in Yellowstone National Park recorded tremor signals potentially triggered by four of the 28 earthquakes for which H17A data were available (Table 1): 20 (Fig. 1), 21 (Fig. 2), 12

(Fig. S1), and 37 (Fig. S2). The tremor signals for earthquake 20 (20 March 2012  $M_w$  7.5 Mexico) are clear, which is also reported in [Pankow and Kilb \(2020\)](#). No tremor-like signals occur within several hours before and after the surface-wave window. Tremor signals detected in the surface-wave windows of earthquakes 12, 21, and 37 are accompanied by comparable tremor-like signals in several hours before and after the windows. Moreover, the tremor signals were not recorded by stations 10–20 km north of H17A, suggesting a shallow, relatively local and possibly nontectonic source for the tremor. Peak dynamic stresses estimated from H17A’s vertical- and transverse-component recordings of the surface waves from earthquake 20 are above 20 kPa, as is also the case for earthquake 37 and two earthquakes that did not trigger tremor in Yellowstone. The majority of the 24 recorded, nontriggering earthquakes produced peak dynamic-stress estimates under 10 kPa. Figure 5 shows that surface waves from all four earthquakes arrived from either the northwest or the southeast, whereas, nontriggering surface waves arrived from these and additional southeast azimuths. Estimated



peak stresses and other attributes for H17A are provided in Table S2 for all earthquakes.

### Observations of triggered earthquakes in central Utah (SRU station)

Station SRU in central Utah recorded 34 of the 38 examined earthquakes, and its seismograms show signals of local earthquakes that were potentially triggered by surface waves from the following seven large earthquakes (Table 2): 21 (Fig. 2), 24 (Fig. S6), 9 (Fig. S3), 10 (Fig. S4), 13 (Fig. S5), and 30 (Fig. S7). Interestingly, peak dynamic stresses inferred from these SRU recordings do not differ substantially from the distribution of peak dynamic stresses inferred from nontriggering teleseismic earthquakes.

We searched for potentially triggered local earthquake signals in seismograms from earthquake 21 (Fig. 6) recorded at stations within about 100 km from the SRU station (Table 2). We observed signals from this local earthquake at seven nearby stations: TMU, CVRU, BCE, PNSU, ROA, DCM, and ARGU, and located its epicenter (Fig. 4). Like those from 21, surface waves from earthquake 24 also triggered a local earthquake in the Raton basin (see [Observations of Triggered Earthquakes in](#)

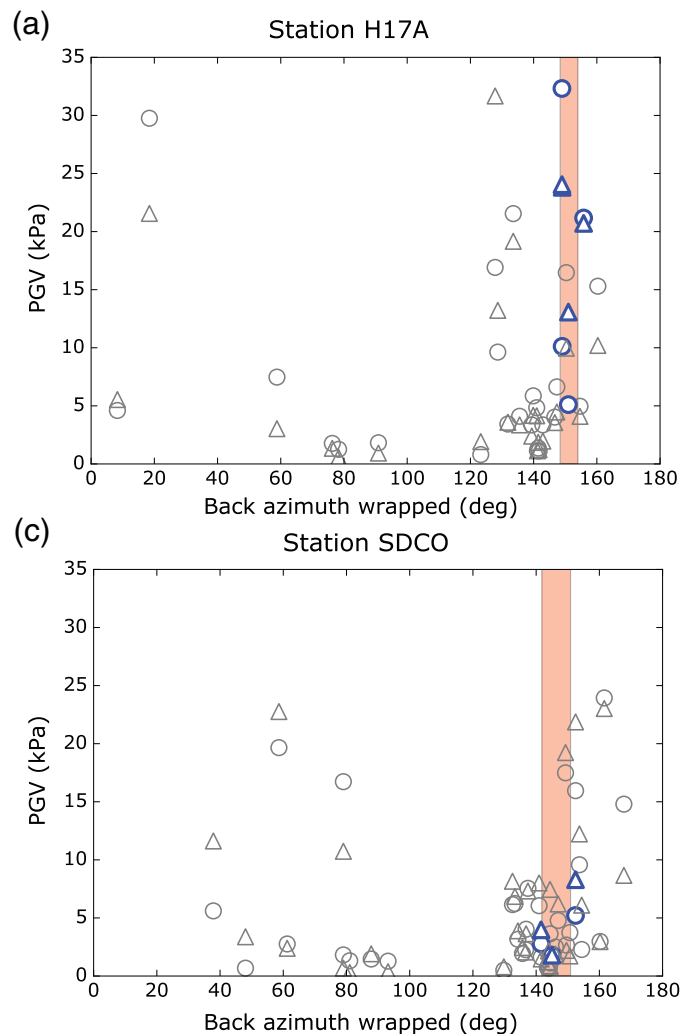


**Figure 5.** Distribution of studied events, as a function of back azimuth (degree). (a) Yellowstone, represented by station H17A; (b) central Utah, represented by station SRU; (c) Raton basin, Colorado, represented by station SDCO. A pair of circle and triangle represents a large global earthquake. The x axis is the estimated peak dynamic stress (in kPa) inferred from Rayleigh waves (circle) and Love waves (triangle), and color symbols representing whether a local event was likely triggered (blue) or not triggered (gray). The back azimuth of each event is wrapped, thus, north ( $0^\circ$ )–south ( $180^\circ$ ), and east ( $90^\circ$ )–west ( $270^\circ$ ) are equivalent. The pink region shows the one standard deviation of triggering azimuths. PGV, peak ground velocity.

[Colorado \(SDCO Station\)](#) section). At the time of earthquake 24, noise levels at H17A (Yellowstone) were too high to detect triggered seismicity signals. The local, SRU-recorded earthquake potentially triggered by earthquake 24 was also recorded by nearby stations ARGU, DCM, and PNSU. Also, during surface wave propagation from earthquakes 9, 10, and 13, signals that could be from local earthquakes were recorded at station SRU. However, other earthquake signals and earthquake-like signals were recorded within hours before and after the surface-wave window. The local earthquake potentially triggered by earthquake 9 was recorded at SRU and seven nearby

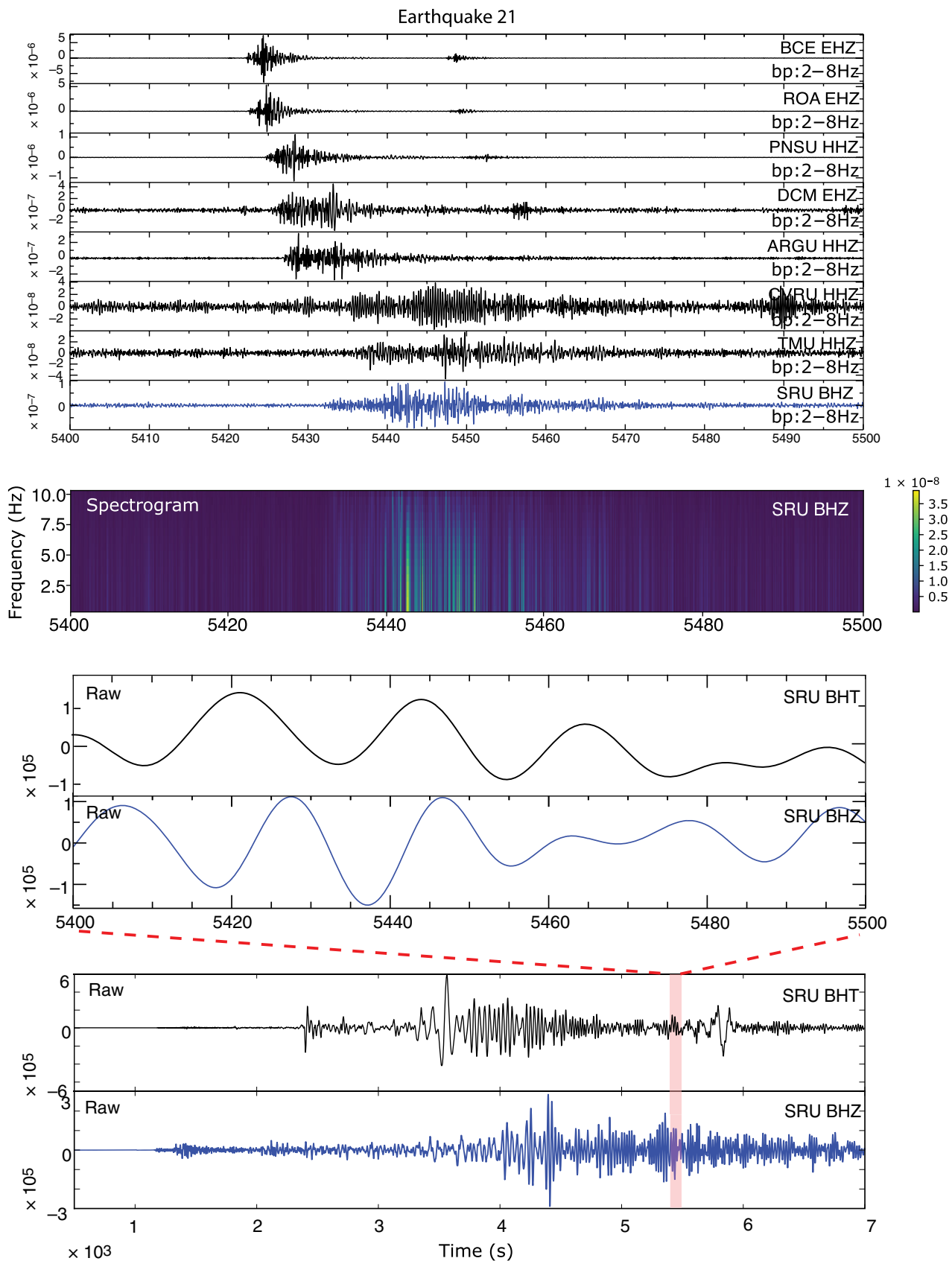


**Figure 6.** Seismograms of earthquake 21 (11 April 2012 v8.6 Sumatra). The layout is the same as in Figure 1, except the top three frames are replaced by a multi-frame panel that represents band-passed vertical-component

seismograms from a group of nearby stations that all recorded a potentially triggered earthquake in central Utah. The color version of this figure is available only in the electronic edition.

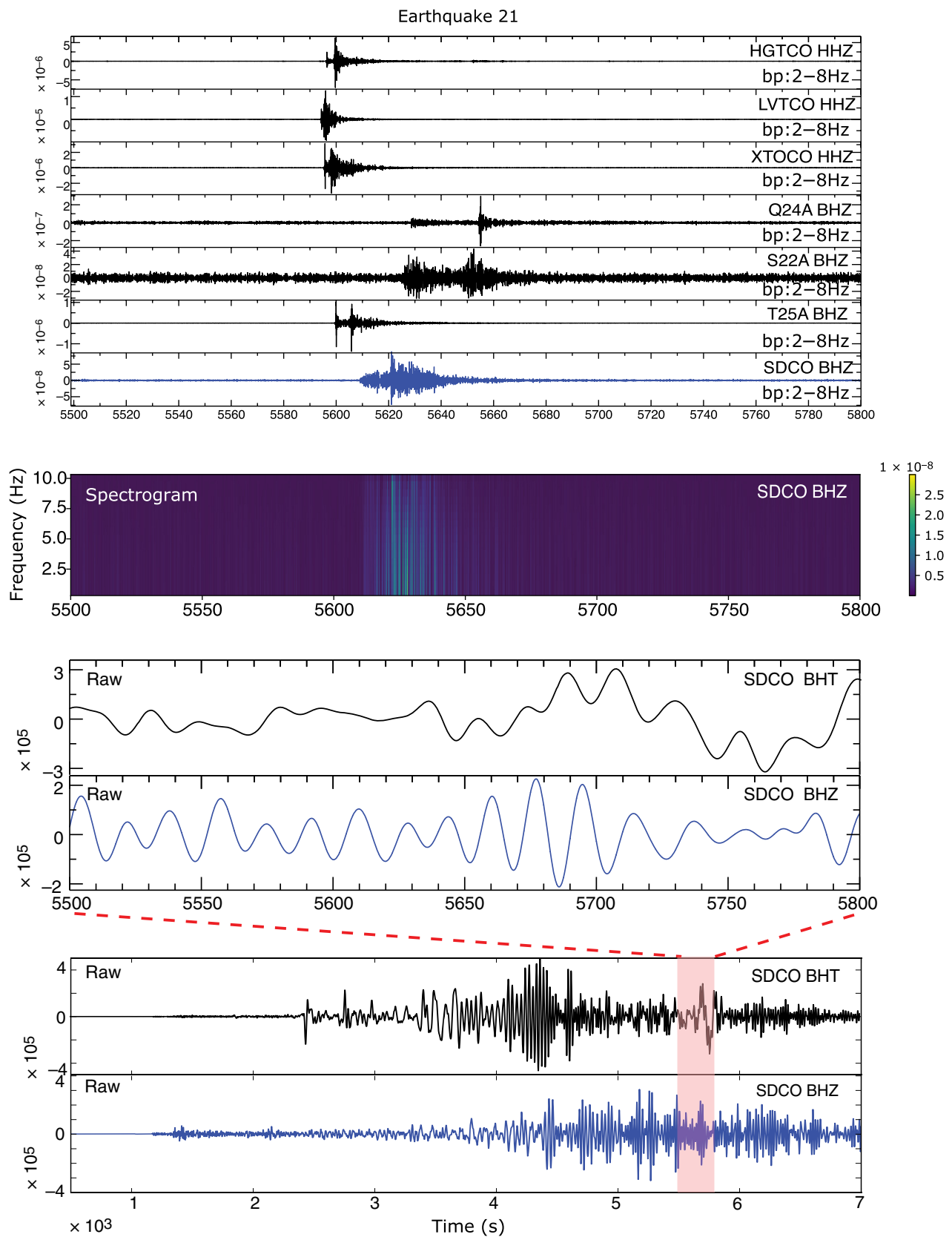


**Figure 7.** Seismograms of possible triggered earthquakes in Colorado following the 11 April 2012  $M_w$  8.6 Sumatra earthquake. Blue seismograms and the spectrogram show the repetitive station SDCO, and black seismograms are represented records from nearby stations. Seismograms of earthquake

21 (11 April 2012  $M_w$  8.6 Sumatra). The layout is the same as in Figure 6. The seismograms shown are from a group of stations that all recorded a potentially triggered earthquake in the Raton basin, Colorado. The color version of this figure is available only in the electronic edition.

TABLE 2

**List of Names of Nearby Station (Right Column) That Recorded Local Earthquakes in Central Utah That Was Potentially Triggered by Some of the Earthquakes from Table 1 (Left Column)**

Number	Date and Origin Time (yyyy/mm/dd hh:mm:ss.s)	Stations
9	2007/08/15 23:41:57.9	SRU, P14A, Q14A, P16A, Q16A, P17A, R17A, Q18A
10	2007/09/12 11:11:15.6	SRU, TMU, Q18A, Q16A, P18A, ROA, P17A, DBD
13	2009/05/28 08:25:04.8	SRU, Q16A, P18A, S18A, P19A, O19A, DUG, Q20A, R20A, O20A, S20A, N20A, N21A, N22A, R24A
21	2012/04/11 08:39:31.4	SRU, TMU, CVRU, BCE, PNSU, ROA, DCM, ARGU
24	2012/09/05 14:42:23.3	SRU, ARGU, DCM, PNSU
30	2014/04/03 02:43:35.9	SRU, ARGU, CVRU, BCE, ROA, BCW, DCM, TMU, EMU, SNO

stations (P14A, Q14A, P16A, Q16A, P17A, R17A, and Q18A), and we picked *P*- and *S*-wave arrivals in these eight records to locate the epicenter of this local earthquake (Fig. 4). Potentially triggered earthquake signals were recorded at seven nearby stations (TMU, Q18A, Q16A, P18A, ROA, P17A, and DBD) from earthquake 10. The local earthquake potentially triggered by earthquake 13 occurs late with respect to the surface-wave window. We picked *P*- and *S*-wave arrivals at 15 nearby stations (stations SRU, Q16A, P18A, S18A, P19A, O19A, DUG, Q20A, R20A, O20A, S20A, N20A, N21A, N22A, and R24A) to locate the epicenter of this local earthquake (Fig. 4).

Earthquake 30 presents an interesting case, as it may have triggered a local earthquake in central Utah not only during the passage of surface waves from earthquake 30, but also, and with higher magnitudes, during the *S*-wave arrival and during the surface-wave window for an  $M_w$  6.5 foreshock, as well as 2 hr earlier and 3 hr later, yielding five local earthquakes in 6 hr of recording. The amplitudes of these local earthquakes suggest that they have magnitudes roughly between 1.0 and 2.0. Background seismicity rates obtained from the USGS in this part of central Utah, combined with the Gutenberg–Richter relationship between earthquake frequency and magnitude, suggest that there should be about 10 earthquakes with magnitudes between 1 and 2 per week. This rate translates to about one such earthquake per 18 hr, definitely raising our five earthquakes in 6 hr as anomalous, with three of these as possibly triggered by teleseismic earthquake 30, and it is  $M_w$  6.5 foreshock.

Station SRU is located at the San Rafael Swell (Delaney and Gartner, 1997) in central Utah, about 100 km east of a roughly north–south-oriented belt of seismicity—the Levan segment of the Wasatch fault—and about 50 km south of a more east–west-oriented lineament of seismicity. Quarry blasts reported by the USGS predominantly occur in the northern part of Utah, more

TABLE 3

**List of Names of Nearby Station (Right Column) That Recorded Local Earthquakes in the Raton Basin, Colorado That Was Potentially Triggered by Some of the Earthquakes from Table 1 (Left Column)**

Number	Date and Origin Time (yyyy/mm/dd hh:mm:ss.s)	Stations
21	2012/04/11 08:39:31.4	SDCO, T25A, Q24A, S22A, XTOCO, HGTCO, LVTCO
23	2012/08/27 04:34:39.5	SDCO, T25A, S22A, Q24A, ANMO, TASL, TASM, KSCO, MVCO, ISCO, AMTX, MSTX, CBKS, OGNE, MNTX, WMOK
24	2012/09/05 14:42:23.3	SDCO

than 50 km from station SRU. However, SRU is about ~20 km southeast of the Cleveland-Lloyd Dinosaur Quarry—an excavation site and open-air museum for dinosaur fossils and, therefore, an unlikely site for strong or frequent blasts. The detected SRU signals typically have strong *S* waves and no preference for the time of day or night at which they occur, further arguing against an anthropogenic source for the signals. During the past 20 yr, the USGS reported about 3000 earthquakes with magnitudes between 2.0 and 3.0 located within a 50 km radius from SRU, which translates to about one such earthquake per week. Therefore, the odds of finding such an earthquake within an ~2000 second long surface wavetrain by chance are about 0.3%, which translates to 3% for earthquakes with magnitudes comparable to the ones we detected ( $1 < M_w < 2$ ). The strongest earthquake in this area had a magnitude of 4.2 during the dodecade spanned by our study. Prior to this, earthquakes were reported to have been dynamically triggered on the Wasatch fault by surface waves from the 2002 Denali fault earthquake (Pankow *et al.*, 2004).

### Observations of triggered earthquakes in Colorado (SDCO station)

Three local earthquakes (Table 3) recorded by station SDCO in Colorado were potentially dynamically triggered, respectively, by teleseismic earthquakes: 21 (Fig. 2), 23 (Fig. S8), and 24 (Fig. 1). Earthquakes 21 and 24 also appear to have triggered local earthquakes in central Utah. The inferred peak dynamic stresses for these recordings (Table S2), again, do not differ substantially from the distribution of peak dynamic stresses inferred from surface waves that did not trigger a local earthquake.

Station SDCO is at the eastern edge of the Colorado plateau and by the northern branch of the Rio Grande rift. The region around SDCO is not, particularly, seismically active. The closest known earthquakes to SDCO are a pair of 2003  $M \sim 3$  earthquakes, 25 km southeast of the station. However, the station is about 80 km northwest of the Raton basin, which has experienced an increase in seismic activity and wastewater injection over the past two decades (Van der Elst *et al.*, 2013; Yeck *et al.*, 2016; Nakai *et al.*, 2017).

For earthquake 21, we observed potentially triggered earthquake signals at seven nearby stations (SDCO, T25A, Q24A, S22A, XTOCO, HGTCO, and LVTGO) and located the epicenter of this local earthquake (Fig. 7).

For earthquake 21 (Fig. 4), the local earthquake signals in Utah arrive about 5430 s after the origin time of earthquake 21, whereas, in Colorado, they arrive about 200 s later, which indicates that the surface waves from earthquake 21 triggered a local earthquake earlier in Utah than in Colorado. Figure 2 shows that these surface waves propagated roughly from northwest to southeast in the western United States and would have indeed needed about 200 s to travel from station SRU in Utah to station SDCO in Colorado. This evidence suggests that these earthquakes in Utah and Colorado are indeed dynamically triggered by the same component of the wavefield, rather than coincident earthquakes.

Earthquake 23 produced the local earthquake signal with the largest amplitude and was observed by the most nearby stations. It was observed at 17 stations (SDCO, T25A, S22A, Q24A, ANMO, TASL, TASM, KSCO, MVCO, ISCO, AMTX, MSTX, CBKS, OGNE, SRU, MNTX, and WMOK). Using *P*- and *S*-wave picks, we located the epicenter of this earthquake to be in the Raton basin (Fig. 4). The local earthquake potentially triggered by teleseismic earthquake 24 was observed only at SDCO with an order of magnitude lower amplitudes than for earthquake 23 and relatively late in the surface wavetrain.

## PREVAILING CONDITIONS FOR DYNAMIC TRIGGERING

Despite searching systematically through over a 1000 continentwide seismograms from one earthquake (21) and hundreds of seismograms recorded in three particularly interesting intraplate regions from the 38 largest earthquakes of the dodecade spanned by our study, we found little evidence for the dynamic triggering of tectonic tremor and earthquakes. Even in the three intraplate regions where we did detect potentially triggered seismicity, there are no obvious patterns as to when triggering occurs and when it does not. Meanwhile, our study is not alone in attempts to detect intraplate triggering (Velasco *et al.*, 2008, 2016; Van der Elst *et al.*, 2013; Bockholt *et al.*, 2014) and detections of dynamically triggered seismicity at plate boundaries continue to accumulate (Canitano *et al.*, 2019). We, therefore, explore the prevailing conditions under which dynamic triggering occurs.

In Figure 5, for potentially dynamically triggered local earthquakes in both central Utah and the Raton basin, it is possible that triggering is facilitated when surface waves arrive from two favorable back azimuths, 180° apart, though our detections are nowhere near numerous enough to claim statistical significance. Back azimuth might also contribute to triggering tremor in Yellowstone, as a secondary factor after dynamic stresses.

Besides the analysis of back azimuth in Figure 5, we further evaluate and assign values (Table S2) for the following set of

parameters to each seismogram: estimated peak stress inferred from the PGV estimated from vertical-component seismograms (PGVZ), estimated peak stress inferred from the PGV estimated from transverse-component seismograms (PGVT), local time of the day of surface-wave arrival normalized to 0 being around midnight and 1 being around midday (TOD), and vertical ground velocity resulting from solid-Earth tides computed with the method of Milbert (2015; TIDE; see Data and Resources).

From Figure 8a, we determined a stress threshold of 10 kPa for triggering tremor in Yellowstone. About 20 of the 24 examples not associated with triggering had PGVT values below 10 kPa, suggesting that stresses imposed by Love waves play a decisive role in triggering tremor here, whichever its nature. Hill *et al.* (2013) suggest that, specifically for the San Andreas fault near Parkfield, California, Rayleigh waves modulate tremor via pore-pressure fluctuations, but that the fault slip associated with the tremor is caused by *SH* and Love waves polarized largely perpendicular or parallel to the San Andreas fault. Figure 5 confirms this notion and shows that the back azimuths for earthquakes that triggered tremor are either somewhat aligned or at right angles with the San Andreas fault's strike. Meanwhile, our analysis of potentially dynamically triggered local earthquakes in Colorado and Utah shows that these earthquakes occur independently of peak stress values estimated from surface waves. In addition, we did not find any obvious correlation between TOD, TIDE, and dynamic triggering.

## DISCUSSION

In a search for seismic events, possibly triggered by Love waves from a powerful teleseismic earthquake, in all of the conterminous United States, we confirmed the notion that seismic events are predominantly triggered in regions of high-tectonic and seismic activity (the westernmost boundary of the North American tectonic plate). Within USArray data from earthquake 21 (2012  $M_w$  8.6 Sumatra), we did not find signals of triggered seismic events in the CEUS, which is consistent with its plate-tectonic inactivity. Consistent with these end-member findings of lots of triggered activity along the west coast and little in tectonically stable North America, we found a small number of seismic events, likely triggered by earthquake 21 and other teleseismic earthquakes, in three locations in the western U.S. interior that are less seismically active than the plate boundary. Specifically, we newly detected up to four potentially triggered tremor bursts in Yellowstone, up to seven potentially triggered earthquakes in Utah, as well as three potentially triggered earthquakes in the Raton basin, Colorado from an examination of seismograms from 38 large teleseismic earthquakes (Table 1).

Like earthquake 21 (2012  $M_w$  8.6 Sumatra), earthquakes 17, 22, 27, and 36 also generated Love waves that were stronger than Rayleigh waves. Therefore, we also searched for signals from local earthquakes or tremor in the surface-wave windows of all USArray seismograms recorded in the CEUS from these

four earthquakes. We did not detect signals from local earthquakes or tremor in these records. We thus confirm that Love waves do not appear to trigger seismicity in the CEUS, consistent with its plate-tectonic inactivity, and perhaps indicating the absence of stressed strike-slip faults.

Dynamically triggered events are hard to detect in raw seismograms, their identification can be negatively affected by various types of noise, including anthropogenic seismic noise (Diaz *et al.*, 2017; Marcillo and MacCarthy, 2020), and instrumental quirks or adjustments, such as mass centerings or calibrations, or might coincide with, large earthquakes' surface waves, rather than be triggered by them. For example, upon the first examination, we observed two candidate-triggered earthquakes in Minnesota after earthquake 21. A subsequent closer inspection did not reject the candidate-triggered events, because the signals shared characteristics with triggered earthquake signals. However, after inspection of hours and days of seismograms before and after the earthquake, we rejected both the candidates, because a multitude of similar signals, possibly, from anthropogenic events, implied a high likelihood for one of these events coinciding with the earthquake's surface waves by chance. Through the use of visual inspection, in addition to, timing- and frequency-based selection criteria for these seismic phenomena, our search yielded numerous false positives, illustrating the challenge posed by moving from ad hoc observations of dynamic triggering to a systematic search that also includes a catalog of teleseismic events that did not dynamically trigger other events, even when large stress variations were supplied.

Table 1 presents the 38 teleseismic earthquakes used in our study, up to 11 of which produced potentially triggered events in three western intraplate regions. Our observations and analyses confirm that tremor is more likely triggered by high dynamic-stress surface waves, consistent with the literature. Our results also indicate that triggered earthquakes are not positively correlated with high dynamic stress surface waves, in agreement with Wang *et al.* (2019) and Alfaro-Diaz *et al.* (2020). On the contrary, our analysis shows that back azimuth appears to be an important factor in dynamic triggering for both earthquakes (as also shown in Alfaro-Diaz *et al.*, 2020) as well as tremor. A large number of surface waves (Table S2) with favorable back azimuths (Fig. 5) are not associated with triggering, which argues for future multiparameter analyses, including stress values estimated at depth within the crust, all components of the dynamic-stress tensors from largely coeval Love and Rayleigh waves, and how dynamic-stress tensors translate to stress quantities (other than peak stress estimates) that matter to faulting.

Our analysis (Figs. 5 and 8) shows that a data set of likely triggered events has provided us with several insights:

1. Prevailing conditions for triggering tremor in Yellowstone include peak stresses estimated from Love waves exceeding a stress threshold of just over 10 kPa.

2. The arrival azimuth of surface waves appears to be important in whether surface waves can trigger local tremor and earthquakes.
3. Peak dynamic-stress values do not appear to be important for triggering local earthquakes, at least in Utah and Colorado.

## CONCLUSIONS

Out of 38 large earthquakes, the surface waves of 11 of them likely triggered seismicity in three intraplate locations in the western United States. One of these earthquakes, the 11 April 2012  $M_w$  8.6 Sumatra earthquake radiated strong Love waves that triggered seismicity in all three locations. We examined each seismogram recorded anywhere in the conterminous United States of this earthquake and did not find dynamically triggered events in the CEUS. However, we found several dozens of records of dynamically triggered events along the western edge of the North American plate, which align with previous reports in the literature. In total, from all 38 earthquakes, we report eight small, local earthquakes (in Utah or Colorado) and four cases of tremor in Yellowstone that are likely triggered by surface waves from these teleseismic earthquakes.

Reports about dynamically triggered seismic events are regularly published in the professional literature (Freed, 2005; Gonzalez-Huizar *et al.*, 2012; Aiken and Peng, 2014; Johnson *et al.*, 2015; Yao *et al.*, 2015; Bansal *et al.*, 2016, 2018; Opris *et al.*, 2018; Prejean and Hill, 2018; Wang *et al.*, 2019), yet many aspects about the physical mechanisms leading to such triggering remain elusive. Documenting instances of dynamically triggered seismic events and the conditions under which they occur and not occur provide us with data to illuminate some of these aspects. In this article, we approached this challenge from multiple different perspectives:

1. Dynamically triggered tremor was newly detected in the Yellowstone hotspot region, which could be hydrothermal in origin, and dynamically triggered earthquakes were newly detected in central Utah and southeastern Colorado, near the Raton basin.
2. We found that the back azimuth of surface waves could be an important factor in dynamic triggering.
3. Peak dynamic stresses from Love waves that appear to have triggered tremor in Yellowstone exceed 10 kPa.
4. Our analysis further revealed that peak dynamic stresses estimated from teleseismic surface waves do not appear to correlate with whether or not a local earthquake is triggered.
5. Love waves from five large earthquakes do not appear to trigger seismicity in the CEUS.

## DATA AND RESOURCES

All seismic data were downloaded through the Incorporated Research Institutions for Seismology (IRIS) Wilber 3 system (<http://ds.iris.edu/>)

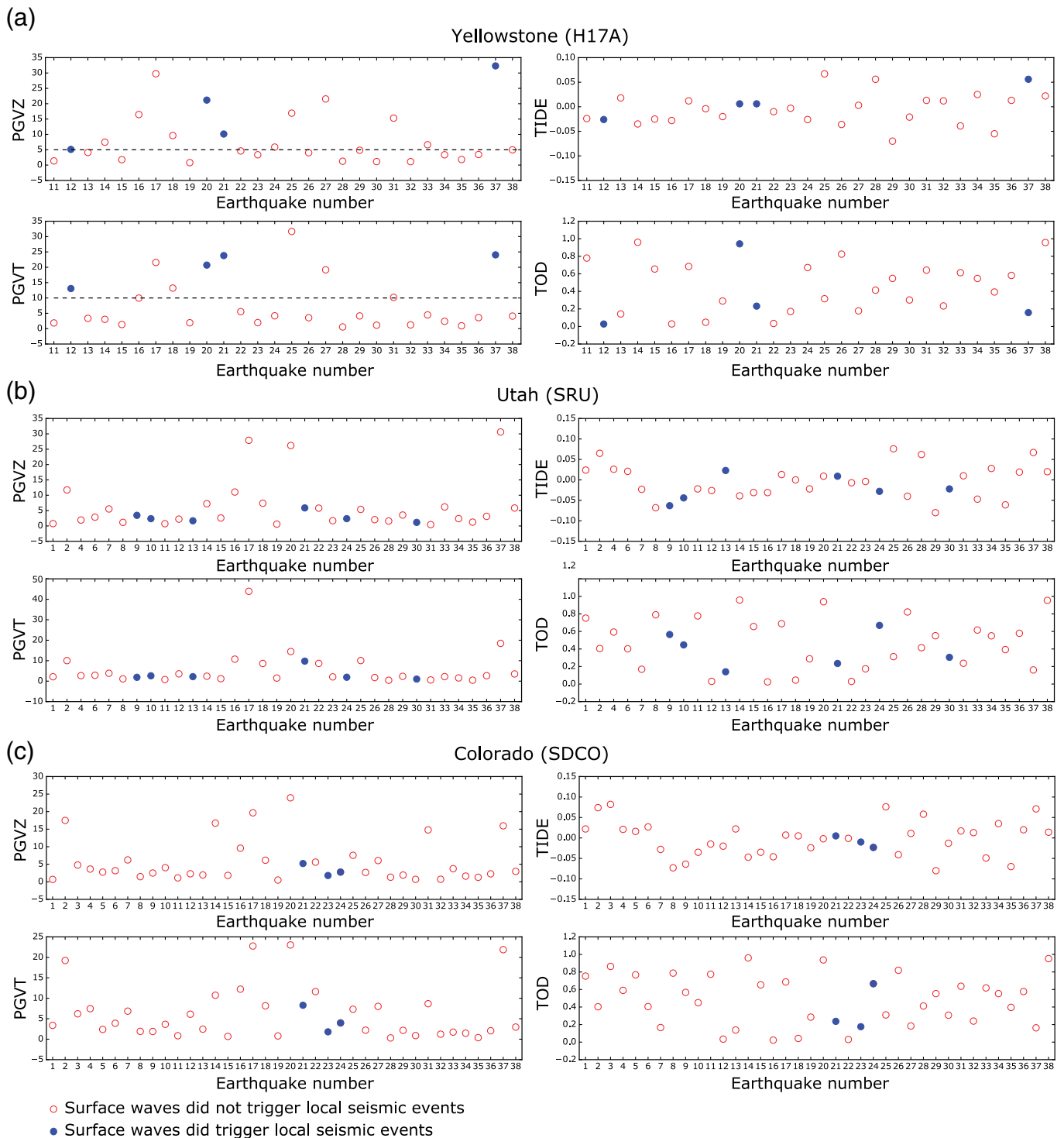


**Figure 8.** Visualization results for the three intraplate regions: (a) Yellowstone, represented by station H17A, (b) central Utah, represented by station SRU, and (c) the Raton Basin, Colorado, represented by station SDCO. Blue dot and red circle represent surface waves that either did or did not trigger local seismic events. The  $x$  axis shows the number of earthquakes in Table 1, and the  $y$  axis is one of the parameters. The dashed line indicates the threshold for separating triggered seismic events. Parameters names: PGVT, estimated peak stress inferred from the PGV

estimated from transverse-component seismograms; PGVZ, estimated peak stress inferred from the PGV estimated from vertical-component seismograms; TIDE, vertical ground velocity resulting from solid-Earth tides computed with the method of Milbert (2015); TOD, local time of the day of surface-wave arrival normalized to 0 being around midnight and 1 being around midday. The color version of this figure is available only in the electronic edition.

wilber3/find\_event, last accessed September 2019) or IRIS Web Services, including the following seismic networks (<http://ds.iris.edu/mda>, last accessed April 2020): (1) the AZ (ANZA; UC San Diego, 1982); (2) the TA (Transportable Array; Incorporated Research Institutions for Seismology (IRIS) Transportable Array, 2003); (3) the US (U.S. National Seismograph Network [USNSN]; Albuquerque Seismological Laboratory (ASL)/USGS, 1990); (4) the IU (Global Seismographic Network [GSN]; Albuquerque Seismological Laboratory (ASL)/U.S. Geological Survey (USGS), 1988); (5) the BK (Berkeley Digital Seismic Network [BDSN]; Northern California Earthquake Data Center [NCEDC], 2014); (6) the CI (Southern California Seismic Network [SCSN]; California Institute of Technology and United States Geological Survey Pasadena, 1926); (7) the XI (Superior Province Rifting EarthScope Experiment [SPREE]; Van der Lee *et al.*, 2011); (8) the II (GSN; Scripps Institution of Oceanography [SIO], 1986); (9) the NN (University of Nevada, Reno, 1971); (10) the UO (University of Oregon and Pacific Northwest Seismic Networks [UOPNSN]; University of Oregon, 1990); (11) the UW (Pacific Northwest Seismic Networks [PNSN]; University of Washington, 1963); (12) the YW (Resolving structural control of episodic tremor and slip along the length of Cascadia [FACES]; Brudzinski and Allen, 2007); (13) the Z9 (Site EffectS Assessment using Ambient Excitations [SESAME]; Fischer *et al.*, 2010); (14) the YX (Flexarray 3D Passive Seismic Imaging of Core-Complex Extension in the Ruby Range Nevada [NE-NV BB]; Klemperer and Miller, 2010); (15) the XQ (Seismic and Geodetic Investigations of Mendocino Triple Junction Dynamics [FAME]; Levander, 2007); (16) the 7A (Mid-Atlantic Geophysical Integrative Collaboration [MAGIC]; Long and Wiita, 2013); (17) the XU (Collaborative Research: EarthScope integrated investigations of Cascadia subduction zone tremor, structure and process [CAFE]; Malone *et al.*, 2006); (18) the XR (Seismic Investigation of Edge Driven Convection Associated with the Rio Grande Rift [SIEDCAR]; Pulliam *et al.*, 2008); (19) the XO (Ozarks–Illinois–Indiana–Kentucky [OIINK]; Pavlis and Gilbert, 2011); (20) the XT (Idaho–Oregon Passive Seismic project [IDOR]; Russo, 2011); and (21) the UU (University of Utah Regional Seismic Network [UURSN]; University of Utah, 1962). Background seismicity rates were obtained from the U.S. Geological Survey (USGS; <https://earthquake.usgs.gov/>, last accessed September 2019). The Advanced National Seismic System (ANSS) earthquake catalog can be accessed at <https://earthquake.usgs.gov/data/comcat/> (last accessed August 2019). Solid tide data can be accessed at <http://geodesyworld.github.io/SOFTS/solid.htm> (last accessed September 2019). Solid earth tide program is written by D. Milbert (2015) (GitHub: <https://github.com/geodesyworld/geodesyworld.github.io>, last accessed September 2019). Supplemental material to this article provides seismograms data of potentially triggered seismic events. It also includes all parameter values for evaluating conditions for dynamic triggering.

## DECLARATION OF COMPETING INTERESTS

The authors acknowledge that there are no conflicts of interest recorded.

## ACKNOWLEDGMENTS

This research is funded by the Integrated Data-Driven Discovery in Geophysical and Astrophysical Sciences (IDEAS) program under

National Science Foundation (NSF) Grant NSF-NRT 1450006, and by Northwestern University's Data Science Initiative (DSI). The authors are grateful to Boris Rösler for stimulating discussions. They also acknowledge the thoughtful and constructive reviews by two anonymous reviewers, Associate Editor Delphine D. Fitzenz, and Editor-in-Chief Thomas L. Pratt.

## REFERENCES

- Aiken, C., and Z. Peng (2014). Dynamic triggering of microearthquakes in three geothermal/volcanic regions of California, *J. Geophys. Res.* **119**, 6992–7009, doi: [10.1002/2014JB011218](https://doi.org/10.1002/2014JB011218).
- Albuquerque Seismological Laboratory (ASL)/U.S. Geological Survey (USGS) (1988). Global Seismograph Network—IRIS/USGS, International Federation of Digital Seismograph Networks, Dataset/Seismic Network, doi: [10.7914/SN/IU](https://doi.org/10.7914/SN/IU).
- Albuquerque Seismological Laboratory (ASL)/U.S. Geological Survey (USGS) (1990). United States National Seismic Network, International Federation of Digital Seismograph Networks, Dataset/Seismic Network, doi: [10.7914/SN/US](https://doi.org/10.7914/SN/US).
- Alfaro-Diaz, R., A. A. Velasco, K. L. Pankow, and D. Kilb (2020). Optimally oriented remote triggering in the Coso geothermal region, *J. Geophys. Res.* **125**, no. 8, Article Number: e2019JB019131, doi: [10.1029/2019JB019131](https://doi.org/10.1029/2019JB019131).
- Bansal, A. R., N. P. Rao, Z. Peng, D. Shashidhar, and X. Meng (2018). Remote triggering in the Koyna-Warna reservoir-induced seismic zone, Western India, *J. Geophys. Res.* **123**, no. 3, 2318–2331, doi: [10.1002/2017JB014563](https://doi.org/10.1002/2017JB014563).
- Bansal, A. R., D. Yao, Z. Peng, and D. Sianipar (2016). Isolated regions of remote triggering in South/Southeast Asia following the 2012  $M_w$  8.6 Indian Ocean earthquake, *Geophys. Res. Lett.* **43**, no. 20, 10,654–10,662, doi: [10.1002/2016GL069955](https://doi.org/10.1002/2016GL069955).
- Bockholt, B. M., C. A. Langston, H. R. De Shon, S. Horton, and M. Withers (2014). Mysterious tremor-like signals seen on the Reelfoot Fault, northern Tennessee, *Bull. Seismol. Soc. Am.* **104**, no. 5, 2194–2205, doi: [10.1785/0120140030](https://doi.org/10.1785/0120140030).
- Brodsky, E. E., and N. J. van der Elst (2014). The uses of dynamic earthquake triggering, *Annu. Rev. Earth Planet. Sci.* **42**, no. 1, 317–339, doi: [10.1146/annurev-earth-060313-054648](https://doi.org/10.1146/annurev-earth-060313-054648).
- Brudzinski, M., and R. Allen (2007). Resolving structural control of episodic tremor and slip along the length of Cascadia, International Federation of Digital Seismograph Networks, Dataset/Seismic Network, doi: [10.7914/SN/YW\\_2007](https://doi.org/10.7914/SN/YW_2007).
- California Institute of Technology and United States Geological Survey Pasadena (1926). Southern California Seismic Network, International Federation of Digital Seismograph Networks, Dataset/Seismic Network, doi: [10.7914/SN/CI](https://doi.org/10.7914/SN/CI).
- Canitano, A., H. Gonzalez-Huizar, Y. J. Hsu, H. M. Lee, A. T. Linde, and S. Sacks (2019). Testing the influence of static and dynamic stress perturbations on the occurrence of a shallow, slow slip event in eastern Taiwan, *J. Geophys. Res.* **124**, no. 3, 3073–3087.
- Castro, R. R., R. Clayton, E. Hauksson, and J. Stock (2017). Observations of remotely triggered seismicity in Salton Sea and Coso geothermal regions, Southern California, USA, after big ( $M_w > 7.8$ ) teleseismic earthquakes, *Geophys. Int.* **56**, no. 3, 269–286.
- Castro, R. R., H. Gonzalez-Huizar, F. R. Zúñiga, V. M. Wong, and A. A. Velasco (2015). Delayed dynamic triggered seismicity in northern Baja California, México caused by large and remote

- earthquakes, *Bull. Seismol. Soc. Am.* **105**, no. 4, 1825–1835, doi: [10.1785/0120140310](https://doi.org/10.1785/0120140310).
- Cerda, I., H. Gonzalez-Huizar, A. A. Velasco, D. L. Kilb, and K. L. Pankow (2011). Systematic analysis of dynamic earthquake triggering using the EarthScope's USArray data, *Eos Trans. AGU, Fall Meet. Suppl.*, Abstract Number S13A-2258.
- Chao, K., and K. Obara (2016). Triggered tectonic tremor in various types of fault systems of Japan following the 2012  $M_w$  8.6 Sumatra earthquake, *J. Geophys. Res.* **121**, no. 1, 170–187, doi: [10.1002/2015JB012566](https://doi.org/10.1002/2015JB012566).
- Chao, K., and C. Yu (2018). A MATLAB GUI for examining triggered tremor: A case study in New Zealand, *Seismol. Res. Lett.* **89**, no. 6, 2362–2373, doi: [10.1785/0220180057](https://doi.org/10.1785/0220180057).
- Chao, K., Z. Peng, A. Fabian, and L. Ojha (2012). Comparisons of triggered tremor in California, *Bull. Seismol. Soc. Am.* **102**, no. 2, 900–908, doi: [10.1785/0120110151](https://doi.org/10.1785/0120110151).
- Chao, K., Z. Peng, W. B. Frank, G. A. Prieto, and K. Obara (2019). Isolated triggered tremor spots in South America and implications for global tremor activity, *Seismol. Res. Lett.* **90**, no. 5, 1726–1739, doi: [10.1785/0220190009](https://doi.org/10.1785/0220190009).
- Chao, K., Z. Peng, H. Gonzalez-Huizar, C. Aiken, B. Enescu, H. Kao, A. A. Velasco, K. Obara, and T. Matsuzawa (2013). A global search for triggered tremor following the 2011  $M_w$  9.0 Tohoku earthquake, *Bull. Seismol. Soc. Am.* **103**, no. 2B, 1551–1571.
- Chao, K., Z. Peng, Y.-J. Hsu, K. Obara, C. Wu, K.-E. Ching, S. van der Lee, H.-C. Pu, P.-L. Leu, and A. Wech (2017). Temporal variation of tectonic tremor activity in southern Taiwan around the 2010  $M_L$  6.4 Jiashian earthquake, *J. Geophys. Res.* **122**, no. 7, 5417–5434, doi: [10.1002/2016JB013925](https://doi.org/10.1002/2016JB013925).
- Delaney, P. T., and A. E. Gartner (1997). Physical processes of shallow mafic dike emplacement near the San Rafael Swell, Utah, *Geol. Soc. Am. Bull.* **109**, no. 9, 1177–1192, doi: [10.1130/0016-7606\(1997\)109<1177:PPOSMD>2.3.CO;2](https://doi.org/10.1130/0016-7606(1997)109<1177:PPOSMD>2.3.CO;2).
- Díaz, J., M. Ruiz, P. S. Sánchez-Pastor, and P. Romero (2017). Urban seismology: On the origin of earth vibrations within a city, *Sci. Rep.* **7**, no. 1, 1–11.
- Fischer, K. M., R. B. Hawman, and L. S. Wagner (2010). Southeastern suture of the Appalachian margin experiment, International Federation of Digital Seismograph Networks, Dataset/Seismic Network, doi: [10.7914/SN/Z9\\_2010](https://doi.org/10.7914/SN/Z9_2010).
- Freed, A. M. (2005). Earthquake triggering by static, dynamic, and postseismic stress transfer, *Annu. Rev. Earth Planet. Sci.* **33**, no. 1, 335–367, doi: [10.1146/annurev.earth.33.092203.122505](https://doi.org/10.1146/annurev.earth.33.092203.122505).
- Gomberg, J., and S. Prejean (2013). Triggered tremor sweet spots in Alaska, *J. Geophys. Res.* **118**, no. 12, 6203–6218, doi: [10.1002/2013JB010273](https://doi.org/10.1002/2013JB010273).
- Gomberg, J., J. L. Rubinstein, and Z. Peng (2008). Widespread triggering of nonvolcanic tremor in California, *Science* **319**, 173, doi: [10.1126/science.1149164](https://doi.org/10.1126/science.1149164).
- Gonzalez-Huizar, H., A. A. Velasco, Z. Peng, and R. Castro (2012). Remote triggered seismicity caused by the 2011,  $M_9.0$  Tohoku, Japan earthquake, *Geophys. Res. Lett.* **39**, L10302, doi: [10.1029/2012GL051015](https://doi.org/10.1029/2012GL051015).
- Hill, D. P. (2012). Dynamic stresses, Coulomb failure, and remote triggering—Corrected, *Bull. Seismol. Soc. Am.* **102**, no. 6, 2313–2336, doi: [10.1785/0120120085](https://doi.org/10.1785/0120120085).
- Hill, D. P., and S. G. Prejean (2015). Dynamic Triggering, in *Treatise on Geophysics*, Vol. 4, Elsevier, 273–304.
- Hill, D. P., Z. Peng, D. R. Shelly, and C. Aiken (2013). S-wave triggering of tremor beneath the Parkfield, California, section of the San Andreas fault by the 2011 Tohoku, Japan, earthquake: Observations and theory, *Bull. Seismol. Soc. Am.* **103**, no. 2B, 1541–1550, doi: [10.1785/0120120114](https://doi.org/10.1785/0120120114).
- Huang, H. H., F. C. Lin, B. Schmandt, J. Farrell, R. B. Smith, and V. C. Tsai (2015). The Yellowstone magmatic system from the mantle plume to the upper crust, *Science* **348**, no. 6236, 773–776, doi: [10.1126/science.aaa5648](https://doi.org/10.1126/science.aaa5648).
- Hurwitz, S., R. A. Sohn, K. Luttrell, and M. Manga (2014). Triggering and modulation of geyser eruptions in Yellowstone National Park by earthquakes, earth tides, and weather, *J. Geophys. Res.* **119**, no. 3, 1718–1737.
- Husen, S., S. Wiemer, and R. B. Smith (2004). Remotely triggered seismicity in the Yellowstone National park region by the 2002  $M_w$  7.9 Denali fault earthquake, Alaska, *Bull. Seismol. Soc. Am.* **94**, no. 6B, S317–S331, doi: [10.1785/0120040617](https://doi.org/10.1785/0120040617).
- Incorporated Research Institutions for Seismology (IRIS) Transportable Array (2003). USArray Transportable Array, International Federation of Digital Seismograph Networks, Dataset/Seismic Network, doi: [10.7914/SN/TA](https://doi.org/10.7914/SN/TA).
- Johnson, C. W., and R. Bürgmann (2016). Delayed dynamic triggering: Local seismicity leading up to three remote  $M \geq 6$  aftershocks of the 11 April 2012  $M$  8.6 Indian Ocean earthquake, *J. Geophys. Res.* **121**, no. 1, 134–151, doi: [10.1002/2015JB012243](https://doi.org/10.1002/2015JB012243).
- Johnson, C. W., R. Bürgmann, and F. F. Pollitz (2015). Rare dynamic triggering of remote  $M \geq 5.5$  earthquakes from global catalog analysis, *J. Geophys. Res.* **120**, no. 3, 1748–1761, doi: [10.1002/2014JB011788](https://doi.org/10.1002/2014JB011788).
- Kato, A., J. I. Fukuda, and K. Obara (2013). Response of seismicity to static and dynamic stress changes induced by the 2011  $M_9.0$  Tohoku-Oki earthquake, *Geophys. Res. Lett.* **40**, no. 14, 3572–3578, doi: [10.1002/grl.50699](https://doi.org/10.1002/grl.50699).
- Klemperer, S., and K. Miller (2010). Flexarray 3D passive seismic imaging of core-complex extension in the Ruby range Nevada, International Federation of Digital Seismograph Networks, Dataset/Seismic Network, doi: [10.7914/SN/YX\\_2010](https://doi.org/10.7914/SN/YX_2010).
- Kundu, B., A. Ghosh, M. Mendoza, R. Bürgmann, V. K. Gahalaut, and D. Saikia (2016). Tectonic tremor on Vancouver Island, Cascadia, modulated by the body and surface waves of the  $M_w$  8.6 and 8.2, 2012 East Indian Ocean earthquakes, *Geophys. Res. Lett.* **43**, no. 17, 9009–9017, doi: [10.1002/2016GL069755](https://doi.org/10.1002/2016GL069755).
- Levander, A. (2007). Seismic and geodetic investigations of Mendocino Triple junction dynamics, International Federation of Digital Seismograph Networks, Dataset/Seismic Network, doi: [10.7914/SN/XQ\\_2007](https://doi.org/10.7914/SN/XQ_2007).
- Linville, L., K. Pankow, D. Kilb, and A. Velasco (2014). Exploring remote earthquake triggering potential across EarthScopes' Transportable Array through frequency domain array visualization, *J. Geophys. Res.* **119**, no. 12, 8950–8963, doi: [10.1002/2014JB011529](https://doi.org/10.1002/2014JB011529).
- Long, M., and P. Wiita (2013). Mid-Atlantic geophysical integrative collaboration, International Federation of Digital Seismograph Networks, Dataset/Seismic Network, doi: [10.7914/SN/7A\\_2013](https://doi.org/10.7914/SN/7A_2013).

- Malone, S., K. Creager, S. Rondenay, T. Melbourne, and G. Abers (2006). Collaborative research: Earthscope integrated investigations of Cascadia subduction zone tremor, structure and process, International Federation of Digital Seismograph Networks, Dataset/Seismic Network, doi: [10.7914/SN/XU\\_2006](https://doi.org/10.7914/SN/XU_2006).
- Marcillo, O. E., and J. MacCarthy (2020). Mapping seismic tonal noise in the contiguous United States, *Seismol. Res. Lett.* **91**, no. 3, 1707–1716, doi: [10.1785/0220190355](https://doi.org/10.1785/0220190355).
- Meng, L., J. P. Ampuero, J. Stock, Z. Duputel, Y. Luo, and V. C. Tsai (2012). Earthquake in a maze: Compressional rupture branching during the 2012  $M_w$  8.6 Sumatra earthquake, *Science* **337**, no. 6095, 724–726, doi: [10.1126/science.1224030](https://doi.org/10.1126/science.1224030).
- Milbert, D. (2015). Solid earth tide program: Solid, *Written in Fortran*, 5, available at <http://geodesyworld.github.io/SOFTS/solid.htm> (last accessed September 2019).
- Nakai, J. S., M. Weingarten, A. F. Sheehan, S. L. Bilek, and S. Ge (2017). A possible causative mechanism of Raton basin, New Mexico and Colorado earthquakes using recent seismicity patterns and pore pressure modeling, *J. Geophys. Res.* **122**, no. 10, 8051–8065, doi: [10.1002/2017JB014415](https://doi.org/10.1002/2017JB014415).
- Northern California Earthquake Data Center (NCEDC) (2014). Berkeley Digital Seismic Network (BDSN), Northern California Earthquake Data Center, doi: [10.7932/BDSN](https://doi.org/10.7932/BDSN).
- Opris, A., B. Enescu, Y. Yagi, and J. Zhuang (2018). Triggering and decay characteristics of dynamically activated seismicity in Southwest Japan, *Geophys. J. Int.* **212**, no. 2, 1010–1021, doi: [10.1093/gji/ggx456](https://doi.org/10.1093/gji/ggx456).
- Pankow, K. L., and D. Kilb (2020). Going beyond rate changes as the sole indicator for dynamic triggering of earthquakes, *Sci. Rep.* **10**, no. 1, 1–12, doi: [10.1038/s41598-020-60988-2](https://doi.org/10.1038/s41598-020-60988-2).
- Pankow, K. L., W. J. Arabasz, J. C. Pechmann, and S. J. Nava (2004). Triggered seismicity in Utah from the 3 November 2002 Denali fault earthquake, *Bull. Seismol. Soc. Am.* **94**, no. 6B, S332–S347, doi: [10.1785/0120040609](https://doi.org/10.1785/0120040609).
- Pavlis, G., and H. Gilbert (2011). Ozark Illinois Indiana Kentucky (OIINK) Flexible Array experiment, International Federation of Digital Seismograph Networks, Dataset/Seismic Network, doi: [10.7914/SN/XO\\_2011](https://doi.org/10.7914/SN/XO_2011).
- Peng, Z., and J. Gomberg (2010). An integrated perspective of the continuum between earthquakes and slow-slip phenomena, *Nature Geosci.* **3**, 599–607, doi: [10.1038/ngeo940](https://doi.org/10.1038/ngeo940).
- Peng, Z., J. E. Vidale, A. G. Wech, R. M. Nadeau, and K. C. Creager (2009). Remote triggering of tremor along the San Andreas fault in central California, *J. Geophys. Res.* **114**, no. B00A06, doi: [10.1029/2008JB006049](https://doi.org/10.1029/2008JB006049).
- Prejean, S. G., and D. P. Hill (2018). The influence of tectonic environment on dynamic earthquake triggering: A review and case study on Alaskan volcanoes, *Tectonophysics* **745**, 293–304, doi: [10.1016/j.tecto.2018.08.007](https://doi.org/10.1016/j.tecto.2018.08.007).
- Prejean, S. G., D. P. Hill, E. E. Brodsky, S. E. Hough, M. J. S. Johnston, S. D. Malone, A. M. O. Pitt, and K. B. Richards-Dinger (2004). Remotely triggered seismicity on the United States west coast following the  $M_w$  7.9 Denali fault earthquake, *Bull. Seismol. Soc. Am.* **94**, no. 6B, S348–S359.
- Pulliam, J., S. Grand, and J. Sansom (2008). Seismic investigation of edge driven convection associated with the Rio Grande Rift, International Federation of Digital Seismograph Networks, Dataset/Seismic Network, doi: [10.7914/SN/XR\\_2008](https://doi.org/10.7914/SN/XR_2008).
- Rösler, B., and S. van der Lee (2020). Using seismic source parameters to model frequency-dependent surface-wave radiation patterns, *Seismol. Res. Lett.* **91**, 992–1002, doi: [10.1785/0220190128](https://doi.org/10.1785/0220190128).
- Rubinstein, J. L., J. Gomberg, J. E. Vidale, A. G. Wech, H. Kao, K. C. Creager, and G. Rogers (2009). Seismic wave triggering of nonvolcanic tremor, episodic tremor and slip, and earthquakes on Vancouver Island, *J. Geophys. Res.* **114**, no. B00A01, doi: [10.1029/2008JB005875](https://doi.org/10.1029/2008JB005875).
- Russo, R. (2011). Deformation and magmatic modification of a steep continental margin, Western ID-Eastern OR, International Federation of Digital Seismograph Networks, Dataset/Seismic Network, doi: [10.7914/SN/XT\\_2011](https://doi.org/10.7914/SN/XT_2011).
- Scripps Institution of Oceanography (SIO) (1986). Global Seismograph Network—IRIS/IDA, International Federation of Digital Seismograph Networks, Dataset/Seismic Network, doi: [10.7914/SN/II](https://doi.org/10.7914/SN/II).
- UC San Diego (1982). ANZA regional network, International Federation of Digital Seismograph Networks, Dataset/Seismic Network, doi: [10.7914/SN/AZ](https://doi.org/10.7914/SN/AZ).
- University of Nevada, Reno (1971). Nevada Seismic Network, International Federation of Digital Seismograph Networks, Dataset/Seismic Network, doi: [10.7914/SN/NN](https://doi.org/10.7914/SN/NN).
- University of Oregon (1990). University of Oregon and Pacific Northwest Seismic Network, International Federation of Digital Seismograph Networks, Dataset/Seismic Network, doi: [10.7914/SN/UO](https://doi.org/10.7914/SN/UO).
- University of Utah (1962). University of Utah Regional Seismic Network, International Federation of Digital Seismograph Networks, Dataset/Seismic Network, doi: [10.7914/SN/UU](https://doi.org/10.7914/SN/UU).
- University of Washington (1963). Pacific Northwest Seismic Network, International Federation of Digital Seismograph Networks, Dataset/Seismic Network, doi: [10.7914/SN/UW](https://doi.org/10.7914/SN/UW).
- Vandemeulebrouck, J., P. Roux, and E. Cros (2013). The plumbing of Old faithful Geyser revealed by hydrothermal tremor, *Geophys. Res. Lett.* **40**, no. 10, 1989–1993, doi: [10.1002/grl.50422](https://doi.org/10.1002/grl.50422).
- Van der Elst, N. J., H. M. Savage, K. M. Keranen, and G. A. Abers (2013). Enhanced remote earthquake triggering at fluid-injection sites in the Midwestern United States, *Science* **341**, 1380–1385, doi: [10.1126/science.1238948](https://doi.org/10.1126/science.1238948).
- Van der Lee, S., D. Wiens, J. Revenaugh, A. Frederiksen, and F. Darbyshire (2011). Superior Province Rifting Earthscope Experiment, International Federation of Digital Seismograph Networks, Dataset/Seismic Network, doi: [10.7914/SN/XI\\_2011](https://doi.org/10.7914/SN/XI_2011).
- Velasco, A., R. Alfaro-Diaz, and D. Kilb (2016). A time-domain detection approach to identify small earthquakes within the continental United States recorded by the USArray and regional networks, *Bull. Seismol. Soc. Am.* **106**, no. 2, 512–525.
- Velasco, A., S. Hernandez, and T. Parsons (2008). Global ubiquity of dynamic earthquake triggering, *Nature Geosci.* **1**, 375–379, doi: [10.1038/ngeo204](https://doi.org/10.1038/ngeo204).
- Wang, B., R. M. Harrington, Y. Liu, H. Kao, and H. Yu (2019). Remote dynamic triggering of earthquakes in three unconventional Canadian hydrocarbon regions based on a multiple-station matched-filter approach, *Bull. Seismol. Soc. Am.* **109**, no. 1, 372–386.

Yao, D., Z. Peng, and X. Meng (2015). Remotely triggered earthquakes in South-Central Tibet following the 2004  $M_w$  9.1 Sumatra and 2005  $M_w$  8.6 Nias earthquakes, *Geophys. J. Int.* **201**, no. 2, 543–551, doi: [10.1093/gji/ggv037](https://doi.org/10.1093/gji/ggv037).

Yeck, W. L., M. Weingarten, H. M. Benz, D. E. McNamara, E. A. Bergman, R. B. Herrmann, J. L. Rubinstein, and P. S. Earle (2016). Far-field pressurization likely caused one of the largest injection induced earthquakes by reactivating a large pre-

existing basement fault structure, *Geophys. Res. Lett.* **43**, no. 19, 10–198.

---

Manuscript received 2 November 2020

Published online 27 April 2021